Miscible viscous fingering with linear adsorption on the porous matrix

M. Mishra
Nonlinear Physical Chemistry Unit and Center for Nonlinear Phenomena and Complex Systems, Université Libre de Bruxelles (ULB), CP 231, 1050 Brussels, Belgium

M. Martin
Ecole Supérieure de Physique et de Chimie Industrielles, Laboratoire de Physique et Mécanique des Milieux Hétérogènes, PMMH, UMR 7636 CNRS, Université Paris 6, Université Paris 7, 10 rue Vauquelin, 75231 Paris Cedex 05, France

A. De Wit
Nonlinear Physical Chemistry Unit and Center for Nonlinear Phenomena and Complex Systems, Université Libre de Bruxelles (ULB), CP 231, 1050 Brussels, Belgium

(Received 17 January 2007; accepted 2 May 2007; published online 6 July 2007)

Viscous fingering between miscible fluids of different viscosities can affect the dispersion of finite samples in porous media. In some applications, as typically in chromatographic separations or pollutant dispersion in underground aquifers, adsorption onto the porous matrix of solutes (the concentration of which rules the viscosity of the solution) can affect the fingering dynamics. Here, we investigate theoretically the influence of such an adsorption on the stability and nonlinear properties of viscous samples displaced in a two-dimensional system by a less viscous and miscible carrying fluid. The model is based on Darcy's law for the evolution of the fluid velocity coupled to a diffusion-convection equation for the concentration of a solute in the mobile phase inside the porous medium. The adsorption-desorption dynamics of the solute onto the stationary phase is assumed to be at equilibrium, to follow a linear isotherm and is characterized by a retention parameter κ' equal to the adsorption-desorption equilibrium constant K multiplied by the phase ratio F. In practice, retention on the porous matrix renormalizes the log-mobility ratio by a factor $(1+\kappa')$. Correspondingly, a linear stability analysis and nonlinear simulations of the model show that an increase of κ' leads to a stabilization of viscous fingering with fingers appearing on a dimensional time scale multiplied by $(1+\kappa')^3$ and with a dimensional wavelength multiplied by $(1+\kappa')$. © *2007 American Institute of Physics*. [DOI: 10.1063/1.2743610]

I. INTRODUCTION

Miscible viscous fingering is an interfacial fluid flow instability that occurs when a less viscous fluid displaces another more viscous and miscible one in a porous medium, leading to the formation of finger-like patterns at the interface of both fluids. This instability impacts a variety of practical applications of environmental and industrial processes such as the recovery of crude oil from oilfields, filtration and hydrology, fixed-bed chemical processing, and even medical applications.[1] Important characteristics of miscible fingering of one interface such as dispersion curves in the linear regime as well as nonlinear properties of finger growth and merging or tip splitting have been studied theoretically and by numerical simulations.[1–6]

Viscous fingering is also observed in liquid chromatography, which is used to separate the chemical components of a given sample by passing it through a porous medium. Displacement of the sample by a carrying fluid (the eluent) of different viscosity may lead to viscous fingering of either the front or the rear interface of the sample slice, leading to deformation of the initial planar interface. This fingering is detrimental to the separation technique as it contributes to peak broadening and distortions. Such conclusions have been reported by several authors either experimentally[7–12] or numerically.[12–14] Viscous fingering is also of much concern in the dispersion of finite polluted viscous zones inside aquifers.[14–19] In these two applications, the viscous sample is generally of finite width, and adsorption phenomena on the porous matrix can be of importance. Viscous fingering occurs then at the interface where the less viscous fluid displaces the more viscous one, the other interface being stable.[14,15,20,21] Numerical studies of the influence of fingering on dispersion of finite viscous samples has allowed the understanding of the specificities of fingering of such localized viscous zones where the instability is then only a transient phenomenon contributing to widening of the peak.[14,15] However, the effects of solute adsorption and desorption from pores have been largely ignored while modeling the viscous fingering instability, although these phenomena are of critical importance in packed beds and in geological systems, as well as for chromatographic separations. Dickson *et al.* have shown experimentally that solute retention on the porous matrix slows down the growth of viscous fingers and affects the wavelength of the pattern.[11] To our knowledge, no quantitative information or any modeling of this retention influence on fingering has, however, been provided as yet.

In this context, it is the objective of this article to analyze theoretically the influence on miscible viscous fingering of a finite width sample of possible adsorption onto the po-

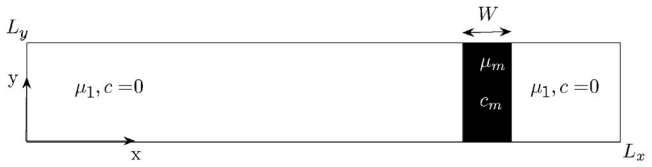

FIG. 1. Sketch of the system at initial time.

rous matrix of a viscosity-controlling solute. We therefore construct a model for miscible viscous fingering incorporating the possibility of adsorption. This model couples Darcy's law for the evolution of the flow field velocity to an equation describing the evolution of the concentration of a solute affecting the viscosity of the solution. This solute is allowed to adsorb-desorb on the porous matrix. A linear adsorption isotherm is assumed as well as rapid equilibrium between the adsorbed and desorbed states. We show here that such retention processes affect not only the characteristic time of the problem but also lower the effective viscosity of the sample and hence modify the viscous fingering properties. Results are presented in terms of a retention parameter κ' quantifying the importance of adsorption processes. A linear stability analysis as well as nonlinear simulations of our model of miscible viscous fingering incorporating adsorption processes are presented to highlight the changes in the quantitative properties of fingering induced by retention.

This article is therefore organized as follows. We first introduce our model of miscible viscous fingering with adsorption in Sec. II. Information derived from a linear stability analysis of this model is discussed in Sec. III, while nonlinear simulations are described in Sec. IV. A conclusion is drawn in Sec. V.

II. MODEL OF VISCOUS FINGERING WITH ADSORPTION

Our model system (see Fig. 1) is a two-dimensional porous medium of length L_x and width L_y in which a sample of viscosity μ_2 containing a solute in concentration $c=c_2$ is injected at an initial time $t=0$. This sample is displaced by its solvent fluid, which has a viscosity μ_1 and in which the solute concentration is $c=0$. The initial length of the sample is W. The displacing fluid is injected uniformly with a mean velocity U along the x direction. We assume that the viscosity of the fluid is an exponential function of c such that

$$\mu(c) = \mu_1 e^{Rc/c_2}, \quad \text{where } R = \ln\frac{\mu_2}{\mu_1}. \tag{1}$$

If $R>0$, then $\mu_1<\mu_2$ and the rear interface of the sample is unstable towards viscous fingering, while the frontal interface is stable and evolves only via dispersion. If $R<0$ the rear interface is stable, while viscous fingering operates at the frontal interface. In this article, we shall focus on the case $R>0$.

A. Adsorption on the porous matrix

Let us now see to what extent these considerations are affected by adsorption of the solute on the porous matrix. To do so, we consider that, once the sample is injected in the porous medium, the solute can adsorb onto the porous matrix following the reversible adsorption-desorption step

$$c_m \underset{k_d}{\overset{k_a}{\rightleftharpoons}} c_s. \tag{2}$$

Here, c_m and c_s are the concentrations of the solute in the mobile and stationary phases, respectively, while k_a and k_d are the respective adsorption and desorption constants. We assume that adsorption on the porous matrix occurs on a time scale much quicker than the characteristic viscous fingering instability one. Hence, we consider that, as soon as the sample is injected into the porous medium, adsorption-desorption phenomena can be considered locally at equilibrium. The validity of this assumption will be addressed in the conclusion once the characteristic time scale of viscous fingering with adsorption will have been derived. Let us then determine the values of c_m and c_s at equilibrium. We know that, at injection, the length of injected sample $L_{\text{inj}} = V_{\text{inj}}/\Phi_{\text{tot}}S$, where V_{inj} is the injected sample volume, S is the cross section of the empty column considered, and Φ_{tot} is the total porosity or void volume fraction. The total number of solute molecules in the sample is

$$n_{\text{tot}} = c_2 V_{\text{inj}} = n_m + n_s, \tag{3}$$

where $n_m = c_{m0}L_{\text{inj}}\Phi_{\text{tot}}S$ and $n_s = c_{s0}L_{\text{inj}}(1-\Phi_{\text{tot}})S$ are the numbers of molecules in the mobile and stationary phase of the sample, respectively, while c_{m0} and c_{s0} are the mobile and stationary phase concentrations, respectively, at equilibrium at initial time. From Eq. (3), we get

$$c_2 V_{\text{inj}} = c_{m0}L_{\text{inj}}\Phi_{\text{tot}}S\left(1 + \frac{c_{s0}}{c_{m0}}\frac{1-\Phi_{\text{tot}}}{\Phi_{\text{tot}}}\right) \tag{4}$$

or also

$$c_2 = c_{m0}(1+\kappa'), \tag{5}$$

where $\kappa' = KF$ is the retention parameter, $F=(1-\Phi_{\text{tot}})/\Phi_{\text{tot}}$ is the phase ratio, while $K=c_{s0}/c_{m0}=k_a/k_d$ is the adsorption-desorption equilibrium constant.

Hence, if the solute is in concentration c_2 in the sample at injection, inside the porous medium the mobile phase concentration of the solute at equilibrium and at initial time is equal to $c_{m0}=c_2/(1+\kappa')$, while the stationary phase concentration is $c_{s0}=Kc_{m0}$. Here we have considered a linear adsorption isotherm characterized by the adsorption-desorption equilibrium constant K and the retention parameter κ'.

As a consequence of the adsorption, the concentration of the solute c_{m0} present in the mobile phase inside the porous system is smaller than the concentration of the solute in the sample before injection. Hence, the effective viscosity of the sample inside the porous matrix is reduced with regard to its initial viscosity μ_2. Inside the porous matrix, we now have, indeed,

$$\mu_m = \mu(c_{m0}) = \mu_1 e^{Rc_{m0}/c_2}. \tag{6}$$

In absence of any retention, $c_{m0}=c_2$, and the viscosity of the injected sample $\mu_2=\mu_1 e^R$ remains the same in the porous medium. In the presence of retention the effective viscosity

of the solution (6), where now the mobile concentration of the solute is only $c_{m0}=c_2/(1+\kappa')$, becomes

$$\mu_m = \mu_1 e^{R/(1+\kappa')}. \tag{7}$$

The log-mobility ratio inside the column with adsorption corresponds to $\ln(\mu_m/\mu_1)=R/(1+\kappa')$, and is therefore reduced by a factor $(1+\kappa')$ with regard to the log-mobility ratio $\ln(\mu_2/\mu_1)=R$ without adsorption.

B. Viscous fingering with adsorption

Let us now construct a model for viscous fingering incorporating the above considerations on adsorption. Assuming the fluid is incompressible and considering Darcy's law to describe the flow inside an isotropic porous medium, the dimensional governing equations for the system considering the mass balance of the solute[22] become

$$\nabla \cdot \mathbf{u} = 0, \tag{8}$$

$$\nabla p = -\frac{\mu(c_m)}{K_p}\mathbf{u}, \tag{9}$$

$$\frac{\partial c_m}{\partial t} + F\frac{\partial c_s}{\partial t} + \mathbf{u}\cdot\nabla c_m = D\nabla^2 c_m, \tag{10}$$

$$\mu(c_m) = \mu_1 e^{Rc_m/c_2} = \mu_1 e^{Rc_m/[c_{m0}(1+\kappa')]}, \tag{11}$$

where K_p is the permeability of the porous medium, p is the pressure, $\mathbf{u}=(u,v)$ is the two-dimensional fluid velocity vector of components u and v along the x and y directions, respectively, while D is the dispersion coefficient.

Considering the linear isotherm adsorption model between the concentrations c_s and c_m as

$$c_s = Kc_m,$$

and recalling that $\kappa'=KF$, Eq. (10) becomes[11,23]

$$(1+\kappa')\frac{\partial c_m}{\partial t} + \mathbf{u}\cdot\nabla c_m = D\nabla^2 c_m, \tag{12}$$

To nondimensionalize the governing equations, we choose the injection speed U as the characteristic velocity and define a length scale $L_c=D/U$ and a time scale $t_c=(1+\kappa')D/U^2$. The nondimensional quantities are then defined as

$$\hat{x}=\frac{x}{L_c}, \quad \hat{y}=\frac{y}{L_c}, \quad \hat{t}=\frac{t}{t_c}, \quad \hat{\mathbf{u}}=\frac{\mathbf{u}}{U},$$

$$p^*=\frac{p}{\mu_1 D/K_p}, \quad \mu^*=\frac{\mu}{\mu_1}, \quad c_m^*=\frac{c_m}{c_{m0}}.$$

Using these dimensionless variables and introducing a moving reference frame

$$x^*=\hat{x}-\hat{t}, \quad y^*=\hat{y}, \quad u^*=\hat{u}-1, \quad v^*=\hat{v}, \quad t^*=\hat{t},$$

the governing equations (8), (9), and (12) with the concentration-dependent viscosity equation (6) become, after dropping the superscripts (*):

$$\nabla \cdot \mathbf{u} = 0, \tag{13}$$

$$\nabla p = -\mu(c_m)(\mathbf{u}+\mathbf{e}_x), \tag{14}$$

$$\frac{\partial c_m}{\partial t} + \mathbf{u}\cdot\nabla c_m = \nabla^2 c_m, \tag{15}$$

$$\mu(c_m) = e^{[R/(1+\kappa')]c_m}, \tag{16}$$

where $\mathbf{e}_x$ is the unit vector along the x direction. Note that this model is the one used classically to describe miscible viscous fingering[2] except for the renormalization of the log-mobility ratio R by a factor $(1+\kappa')$ in Eq. (16). In absence of retention, i.e., when $\kappa'=0$, we shall thus recover classical results of various theoretical studies on viscous fingering.[1–3,5,14,15] While the rescaling of time by a factor $(1+\kappa')$ when retention takes place had already been anticipated qualitatively by Dickson *et al.*,[11] we find thus here that retention, moreover, also rescales the log-mobility ratio R [see Eq. (16)]. This rescaling of R not only affects the onset time of viscous fingering but also the wavelength of the pattern, as we will show in the next section. Let us thus now analyze to what extent adsorption onto the porous matrix of the solute ruling the viscosity of the fluid can affect viscous fingering properties.

III. LINEAR STABILITY ANALYSIS

First we focus on a linear analysis of the stability of the rear interface of the sample with regard to viscous fingering. To do so, we assume that the sample width is large enough for its stability properties at early times to be the same as that of an interface between two semi-infinite region of different viscosities. Equations (13)–(16) are the same as those studied by Tan and Homsy[2] in their linear stability analysis of miscible viscous fingering, except for the $(1+\kappa')$ term. It is hence straightforward to see that, in presence of retention, the analytical dispersion curve (giving the growth rate ω of the perturbations transverse to the front as a function of their wavenumber k) corresponding to a step profile base state at $t=0$ is simply the one obtained analytically by Tan and Homsy [see Eq. (42) of Ref. 2], where R is replaced by $R/(1+\kappa')$:

$$\omega = \frac{1}{2}\left[\left(\frac{R}{1+\kappa'}k-k^2\right) - k\sqrt{k^2+2k\frac{R}{1+\kappa'}}\right]. \tag{17}$$

This admits a most dangerous growth rate

$$\omega_m = \frac{-11+5\sqrt{5}}{8}\left(\frac{R}{1+\kappa'}\right)^2, \tag{18}$$

for the most unstable mode

$$k_m = \frac{\sqrt{5}-2}{2}\left(\frac{R}{1+\kappa'}\right). \tag{19}$$

The dispersion curves (17) are shown in Fig. 2 for different values of the retention parameter κ'. It is observed that, as κ' increases, the effective mobility ratio decreases; consequently, the flow becomes more stable with both the growth

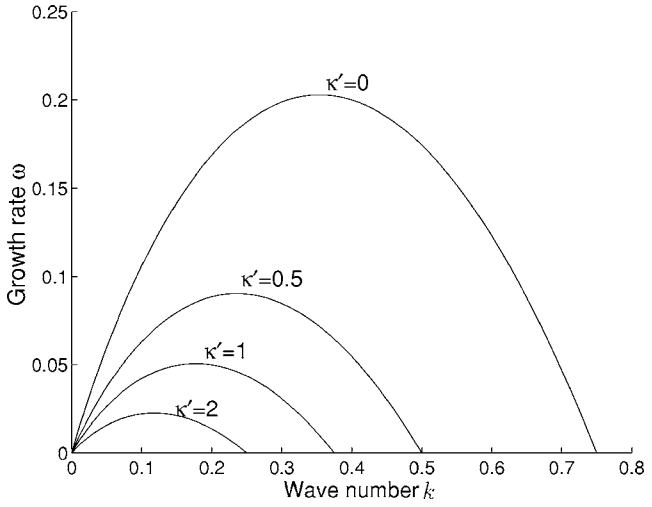

FIG. 2. Dispersion curves giving the growth rate ω of the perturbations as a function of their wavenumber k for $R=3$ and different values of the retention parameter κ'.

rate and the spectrum of unstable wavenumbers becoming smaller. In the absence of adsorption, i.e., $\kappa'=0$, the corresponding dispersion relation (17) is effectively the dispersion relation presented in Tan and Homsy[2] [see their Eq. (42)]. With retention characterized by a constant κ', the dimensionless growth rate is reduced by a factor $(1+\kappa')^2$ while the most unstable wavenumber is smaller by a factor $(1+\kappa')$. In terms of dimensional quantities, it is important to note that the characteristic time scale $t_c=(1+\kappa')D/U^2$ itself depends on κ'.[11] Hence, in dimensional quantities, retention will thus lead to fingers with a dimensional wavelength $\lambda=2\pi L_c/k_m$ larger by a factor $(1+\kappa')$ and appearing on a dimensional time scale $\tau=t_c/\omega_m$ delayed by a factor $(1+\kappa')^3$ with regard to the no-retention case. This conclusion could explain the changes in the properties of viscous fingering induced by retention as observed experimentally by Dickson *et al.*[11] even though quantitative comparison with their results is impossible at this stage as no quantitative information is given on retention parameters in their article.

IV. NONLINEAR SIMULATION

Let us now study the influence of retention in the nonlinear regime. Introducing the stream function $\psi(x,y)$, such that $u=\partial\psi/\partial y$ and $v=-\partial\psi/\partial x$, and following Tan and Homsy,[3] the momentum and concentration equations become

$$\nabla^2\psi = -\frac{d[\ln\mu(c_m)]}{dc_m}\left(\frac{\partial\psi}{\partial x}\frac{\partial c_m}{\partial x}+\frac{\partial\psi}{\partial y}\frac{\partial c_m}{\partial y}+\frac{\partial c_m}{\partial y}\right) = -\frac{R}{1+\kappa'}\left(\frac{\partial\psi}{\partial x}\frac{\partial c_m}{\partial x}+\frac{\partial\psi}{\partial y}\frac{\partial c_m}{\partial y}+\frac{\partial c_m}{\partial y}\right), \tag{20}$$

$$\frac{\partial c_m}{\partial t}+\frac{\partial\psi}{\partial y}\frac{\partial c_m}{\partial x}-\frac{\partial\psi}{\partial x}\frac{\partial c_m}{\partial y}=\frac{\partial^2 c_m}{\partial x^2}+\frac{\partial^2 c_m}{\partial y^2}. \tag{21}$$

Equation (20) is obtained by eliminating the pressure gradient from Darcy's law. Note that in absence of adsorption $(\kappa'=0)$, we recover here again the theoretical model of miscible viscous fingering studied previously by many authors.[3,5,14]

A. Method of solution

Equations (20) and (21) are numerically solved using the pseudospectral method introduced by Tan and Homsy.[3] An operator splitting algorithm is used to solve the convection diffusion equation for the evolution of the concentration by splitting the linear and nonlinear parts separately. The nonlinear advection terms are integrated by implementing a second-order Adams-Bashforth method to provide provisional values for the concentration at each grid points and then the linear dispersion operator is applied to those provisional values. Finally, the solutions are corrected by the trapezoid rule. This code has been validated by reproducing the results of Tan and Homsy.[3]

The boundary conditions are periodic in both x and y directions. In dimensionless units, the width corresponds to a Péclet number $\mathrm{Pe}=UL_y/D$, while $L=UL_x/D$ is the dimensionless length of the two-dimensional domain. The initial dimensionless length of the sample is $l=UW/D$. The initial condition corresponds to a convectionless fluid embedding a rectangular sample of concentration $c_m=1$ of size $\mathrm{Pe}\times l$ in a $c_m=0$ background. The middle of the sample is initially located at $x=4L/5$. For the numerical simulations, the initial condition corresponds to two back-to-back step functions between $c_m=0$ and $c_m=1$ with an intermediate point at which $c_m=1/2+Ar$, where r is a random number between 0 and 1 and A is the amplitude of the noise of the order 10^{-3}. This noise is used to trigger the fingering instability on a reasonable computing time.[14]

B. Discussion of results

Density plots of concentration fields for the parameter values $\mathrm{Pe}=512$, $L=4096$, $l=256$, $R=3$, and various values of the retention parameter κ', are plotted at successive times in Fig. 3, in which the concentration in black and white corresponds to $c_m=1$ and $c_m=0$, respectively. The system is shown in a frame moving with the nondimensional constant speed of the unperturbed solute. Viscous fingering without adsorption, i.e., $\kappa'=0$, is shown in Fig. 3(a) and presents all characteristics of fingering of a finite width sample, as already studied quantitatively in detail before.[14,15] Typically, for $R>0$, the front interface is stable and the rear interface develops fingers, thereby displacing in time the center of gravity of the sample towards the back with respect to its initial position. Figures 3(b)–3(d) correspond to the case when the solute in the injected sample adsorbs (i.e., $\kappa'>0$) onto the porous matrix. It is observed that, in the presence of

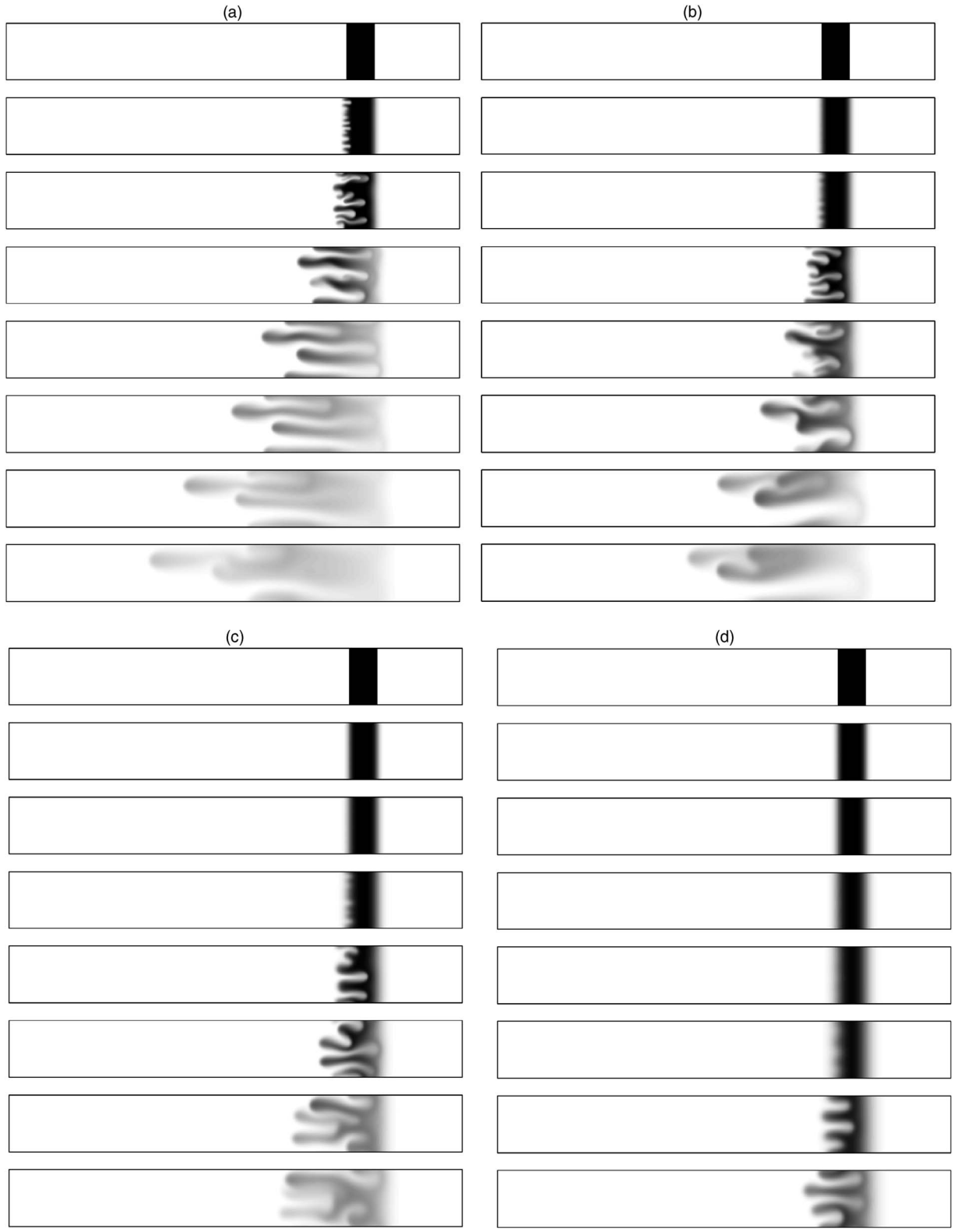

FIG. 3. Density plots of concentration at successive dimensionless times in a frame moving at the velocity of the displaced solute with Pe=512, l=256, R=3 for different values of the retention parameter: (a) $\kappa'=0$, (b) $\kappa'=0.5$, (c) $\kappa'=1$, and (d) $\kappa'=2$. From top to bottom: t=0, 300, 500, 1000, 1500, 2000, 3000, and 4000. The initial condition and the noise used to seed the instability are exactly the same in each case.

adsorption, fingering appears at a later time than for the nonadsorptive case. This result is coherent with the fact that, as κ' increases, the effective log-mobility ratio decreases resulting in a less unstable system. Thus, because of the delay in fingering due to adsorption, fingering might not be observed for example during the transit time across short porous media.

In order to further quantify the influence of adsorption

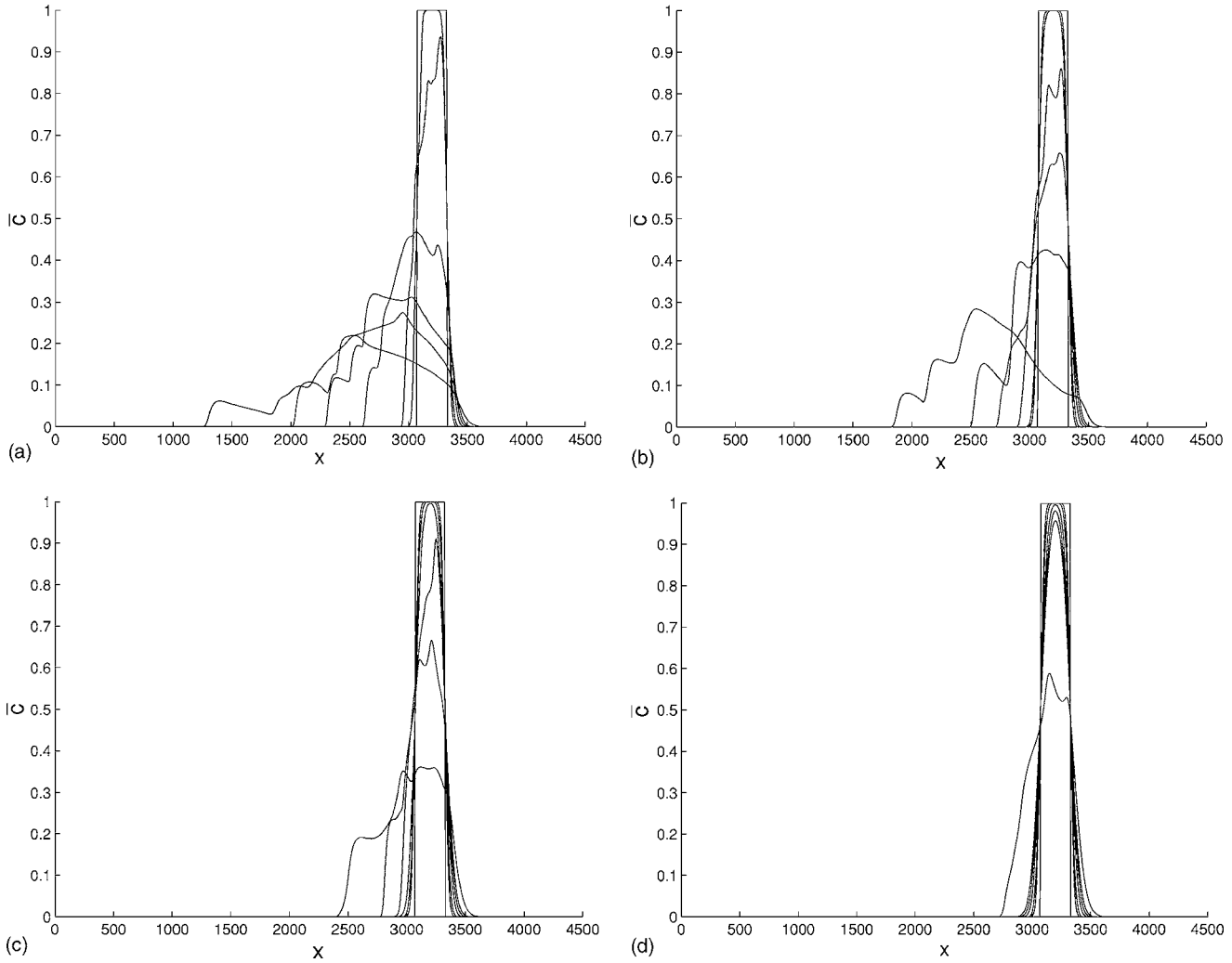

FIG. 4. Transverse averaged concentration profiles corresponding to the dynamics of Fig. 3 shown at successive times $t=0$, 300, 500, 1000, 1500, 2000, and 4000 for different values of the retention parameter: (a) $\kappa'=0$, (b) $\kappa'=0.5$, (c) $\kappa'=1$, and (d) $\kappa'=2$.

on fingering in the nonlinear regime, we plot in Fig. 4 the transverse averaged profiles of concentration defined as

$$\bar{c}(x,t)=\frac{1}{\mathrm{Pe}}\int_0^{\mathrm{Pe}} c_m(x,y,t)dy. \tag{22}$$

Fingering occurs at the rear interface corresponding here to the left front, while the right interface features at early times the standard error function characteristic of simple dispersion. The maximum concentration decreases in time because of dispersion and fingering of the finite sample. Viscous fingering shifts the mean position of the sample towards the back while also widening and distorting the peak.[14] These effects appear at a later time as κ' increases [see Figs. 4(b)–4(d)]. The transverse averaged profiles can next be used to measure the mixing length L_d, which we define here as the length of the interval in which $\bar{c}>0.0001$. Figure 5 displays the temporal variation of this mixing length for various values of the retention parameter κ'. It can be seen that after a diffusive transient, fingering sets in characterized at the beginning by a linear growth of L_d. The onset of fingering is delayed when κ' increases and the slope of the convective growth is also reduced. If we locate the onset time as the time at which the mixing length departs from the diffusive growth, we see that these onset times are roughly $t=400$, 900, 1630, and 3610 for $\kappa'=0$, 0.5, 1, and 2, respectively. This shows that the delay of fingering by a factor $(1+\kappa')^2$ predicted by the linear stability analysis [see Eq. (18)] is recovered in the nonlinear simulations. Comparison between the number of fingers observed at onset on Fig. 3 (typically nine fingers versus six fingers for $\kappa'=0$ or 0.5, respectively) also confirms the predictions of the linear stability analysis; i.e., that the dimensionless wavelength of the fingers is increased by a factor $(1+\kappa')$ in presence of retention.

To quantify the influence of viscous fingering on the distortion of the peak, we compute the variance σ^2 of the averaged profile of concentration $\bar{c}(x,t)$ as

$$\sigma^2(t)=\frac{\int_0^L \bar{c}(x,t)[x-m(t)]^2dx}{\int_0^L \bar{c}(x,t)dx}, \tag{23}$$

where $m(t)=\int_0^L xf(x,t)dx$ is the first moment of $f(x,t)=\bar{c}(x,t)/[\int_0^L \bar{c}(x,t)dx]$, the probability density function of the

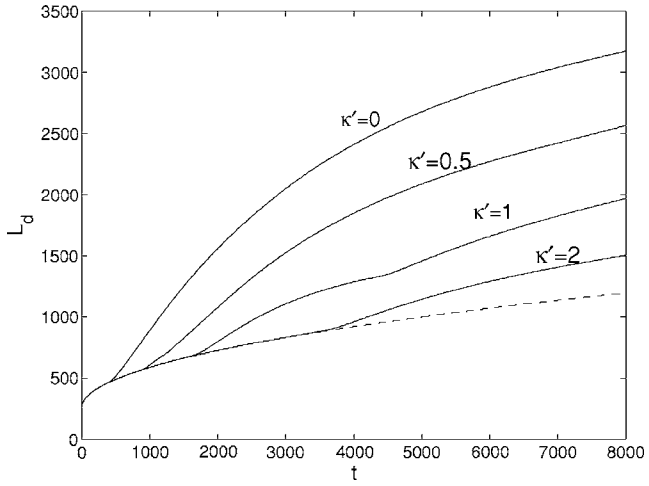

FIG. 5. Mixing length L_d as a function of time for the transverse profiles of Fig. 4. The dashed line shows the diffusive growth of L_d for a stable sample with $R=0$.

continuous distribution $\bar{c}(x,t)$. Figure 6 shows the temporal evolution of the variance which gives the information on the width of the distributions presented in Fig. 4. As already discussed previously,[14] fingering increases the variance of the sample with regard to the case of pure dispersion. In the presence of adsorption (for $\kappa'>0$) a lower variance is found than for the nonadsorptive ($\kappa'=0$) case. We can next extract from the variance the quantity $\sigma_f=\sqrt{\sigma^2-\sigma_o^2}$, which is the contribution of viscous fingering to the variance σ^2. Here, $\sigma_o^2=l^2/12+2t$ is the variance of a stable sample ($R=0$), where the first term corresponds to the contribution due to the initial width l of this sample, while the term linear in t corresponds to the contribution due to dispersive mixing. Figure 7 plots σ_f as a function of time t and of a renormalized time $t/(1+\kappa')^2$, respectively. We see that, as κ' increases at fixed R, the onset time of fingering (corresponding in Fig. 7 to the time at which σ_f departs from zero) is exactly

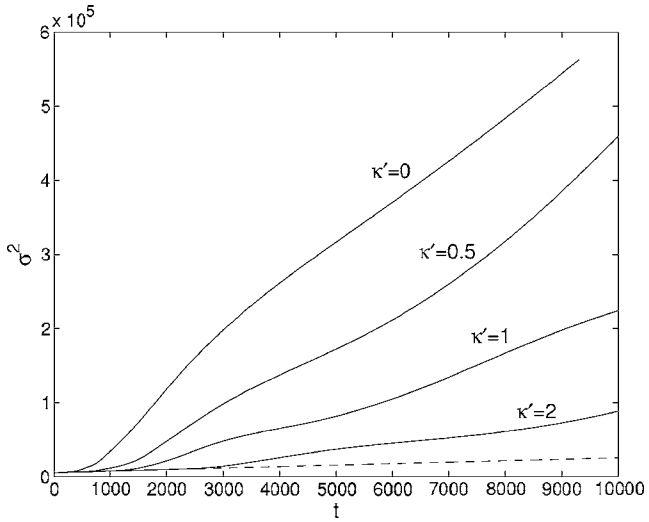

FIG. 6. Variance σ^2 as a function of time for the transverse profiles of Fig. 4. The dashed line shows the variance $\sigma_o^2=l^2/12+2t$ for a stable sample with $R=0$.

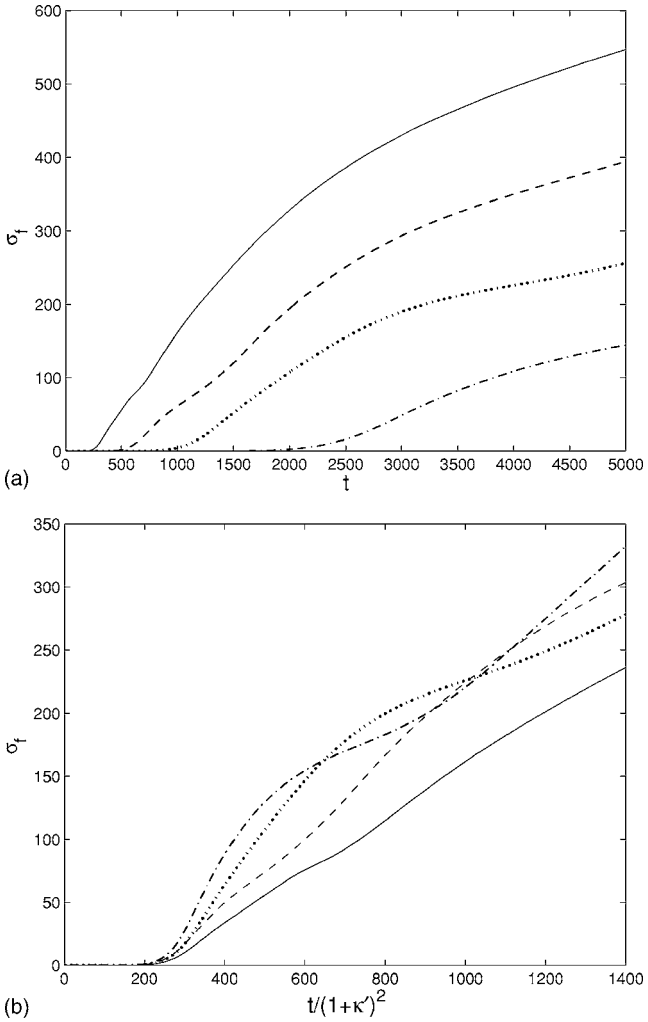

FIG. 7. Contribution σ_f of viscous fingering to the variance as a function of (a) time t and (b) of a renormalized time $t/(1+\kappa')^2$ for the transverse profiles of Fig. 4. The solid, dashed, dotted, and dashed-dotted lines correspond to $\kappa'=0$, 0.5, 1, and 2, respectively.

delayed by a factor $(1+\kappa')^2$ independently of the value of R. Indeed, the different onset times corresponding to t=220, 490, 880, and 1960 for $\kappa'=0$, 0.5, 1, and 2, respectively, in Fig. 7(a), all collapse on the renormalized time $t/(1+\kappa')^2$ used in Fig. 7(b). This is again in good agreement with what has been predicted by the linear stability analysis. We note, moreover, that, in the renormalized time scale, retention leads to a larger contribution of fingering to the variance of the peak, at least just after the onset of fingering.

To gain insight into the nonlinear dynamics of merging and interaction between fingers, we next look at the evolution in time of the power averaged wavenumber $\langle k\rangle$ defined as[5]

$$\langle k(t)\rangle = \frac{\sum_i k_i P_i}{\sum_i P_i}, \tag{24}$$

where k_i are the Fourier modes of the Fourier transform $\hat{c}(k,t)$ of the transverse averaged profile $\langle c(y,t)\rangle = 1/L\int_0^L c_m(x,y,t)dx$ and $P(k)=|\hat{c}(k)|^2$ their amplitude in Fourier space. The averaged wavelength of the fingers is then

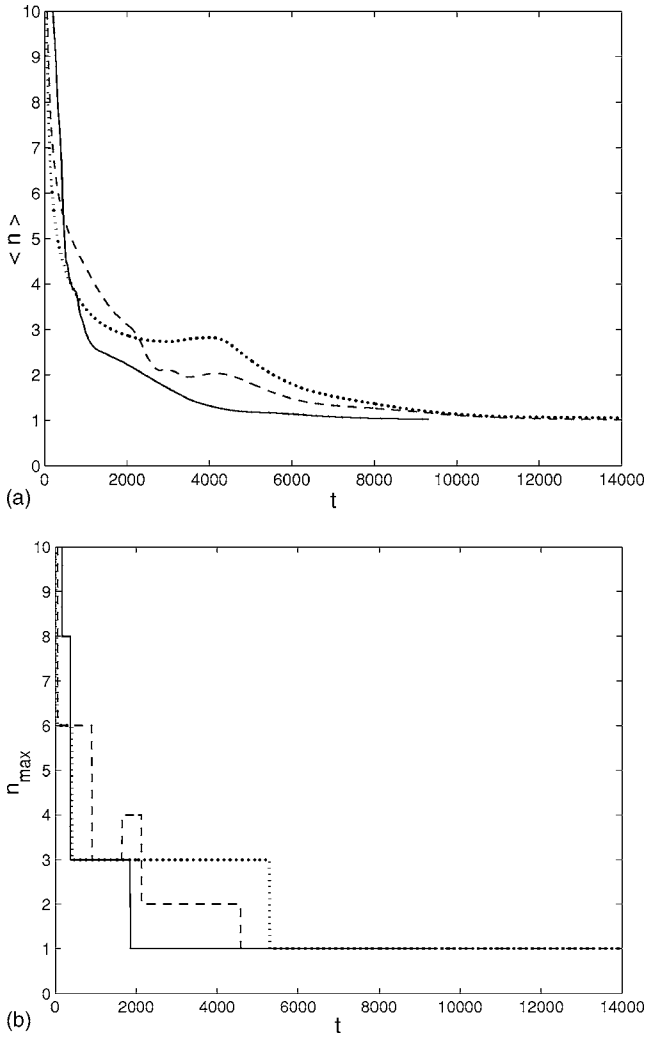

FIG. 8. Dependence on the retention parameter κ' of the temporal variation of (a) the power averaged mean number of fingers $\langle n \rangle$ and (b) the mode of maximum amplitude $n_{\max}$ for the transverse profiles of Fig. 4. The solid, dashed, and dotted lines correspond to $\kappa'=0$, 1, and 2, respectively.

defined as $\langle \lambda(t) \rangle = 2\pi/\langle k(t) \rangle$. The power averaged mean number of fingers in the system is then easily obtained as $\langle n \rangle = \mathrm{Pe}/\langle \lambda(t) \rangle$. As can be seen in Fig. 8(a), this number decreases in time as a consequence of coarsening. A similar information is obtained by looking at the step-like function of Fig. 8(b), which represents simply the $n_{\max}$, the mode of maximum amplitude as a function of time. It can be seen that in the nonlinear regime, coarsening is also delayed when κ' increases.

V. CONCLUSION

The influence of adsorption on the porous matrix of a solute ruling the viscosity of a sample of fluid displaced by a less viscous fluid inside a porous medium has been investigated theoretically. Assuming a linear adsorption isotherm and considering that adsorption-desorption phenomena occur on a characteristic time scale much shorter than that of the fingering instability, we have constructed a simple model coupling Darcy's law for the evolution of the fluid flow velocity to an evolution equation for the key solute concentration. This latter equation incorporates linear adsorption-desorption phenomena through a retention parameter κ'. In the absence of any retention, we recover a classical model describing miscible viscous fingering. In presence of retention, we find that, not only is the characteristic time of the problem changed by a factor $(1+\kappa')$, as had already been anticipated before,[11] but also the log-mobility ratio is divided by a factor $(1+\kappa')$, as effectively part of the solute ruling the viscosity of the solution becomes adsorbed on the porous matrix. As a consequence, fingering is reduced by the adsorption. Quantitatively, this implies that the onset time of the fingering instability is delayed by a factor $(1+\kappa')^2$ and $(1+\kappa')^3$ in dimensionless and dimensional units, respectively. Similarly, the wavelength (both dimensional and dimensionless) of the fingers is larger by a factor $(1+\kappa')$ in presence of retention. These results have been obtained for an isotropic system. Generalization of our results to anisotropic systems in which the ratio between transverse and axial dispersion coefficients is different from 1 is straightforward using the results of the linear stability analysis of Tan and Homsy[2] in a procedure similar to the one sketched here. Let us note that the role of retention has here been studied for one set of representative values of the log-mobility ratio R, Péclet number Pe, and length of the sample l. The effect of changes in these parameters on the viscous fingering pattern in the retained case should be similar to that already studied in the unretained case.[14]

The present results have been obtained assuming that adsorption phenomena can be considered locally at equilibrium as soon as the sample is injected into the porous medium. Let us check the validity of this assumption in chromatographic systems. To do so, we note that the mean adsorption time τ_a in a porous medium made of spherical particles of diameter d_p and having a porosity ϵ can be estimated as the adsorption time in a capillary tube of radius R_c having the same solid surface area per unit liquid volume as the porous medium, i.e., $t_a = R_c^2/4D_m$, where $R_c = d_p\epsilon/3(1-\epsilon)$ and D_m is the molecular diffusion coefficient of the species to be adsorbed. In typical liquid chromatographic columns made of 5 μm particles and having a porosity $\epsilon \sim 0.4$, we get $R_c = 0.22 d_p$. For a typical species with a diffusion coefficient $D_m = 0.5 \times 10^{-9}$ m^2 s^{-1}, this gives $t_a = 6.2 \times 10^{-4}$ s. This time is even about ten times smaller with the recently developed ultrahigh pressure liquid chromatographic columns packed with 1.7 μm particles. This adsorption time can be compared with the characteristic time scale, i.e., $t_c = (1+\kappa')D/U^2$, used to nondimensionalize our model. In typical liquid chromatographic conditions, $D = 1.43 \times 10^{-8}$ m^2 s^{-1} and $U = 1.43 \times 10^{-3}$ m s^{-1} (see Ref. 14). Thus, $t_c = 7.0 \times 10^{-3}$ s. This is more than ten times larger than t_a for $\kappa'=0$, and still more for retained species. In fact, t_a should be compared with the dimensional time scale of appearance of the viscous fingering instability, i.e., $\tau = t_c/\omega_m$, which is proportional to $(1+\kappa')^3/R^2$. τ is therefore the smallest for large R and low κ' values. It is seen in Fig. 2 that for unretained species ($\kappa'=0$) and $R=3$, a quite large value, i.e., in conditions leading to quite small τ values, ω_m is about 0.2; hence, $\tau \sim 35 \times 10^{-3}$ s, which is over 50 times larger than t_a. It can therefore safely be assumed that the adsorption-

desorption process is instantaneously in equilibrium in typical chromatographic columns. If this were not the case, as it might be in some contaminant applications depending on the nature of the soil, then the kinetics of the adsorption process would have to be taken explicitly into account in a more complex model to be developed. In the same spirit, fingering in the presence of nonlinear adsorption could be tackled by a generalization of the model presented here.

To conclude, we note that delay of fingering due to retention should have important consequences for chromatographic applications where adsorption phenomena are present and where viscous fingering is deleterious for the quality of separation. In pollution events in aquifers, we have also shown that an understanding of the adsorption phenomena on the porous matrix is essential if a correct description of the dispersion via fingering of the polluted zone has to be made.

ACKNOWLEDGMENTS

A. De Wit and M. Mishra from ULB thank IRSIB ("Research in Brussels" programme), the Defay Fund and the Communauté française de Belgique (Actions de Recherches Concertées Programme) for financial support. The collaboration between our ULB and ESPCI teams is financially supported by a French (Programme d'Actions Intégrées no. 08948YD) - Belgian (CGRI) Tournesol grant.

[1] G. M. Homsy, "Viscous fingering in porous media," Annu. Rev. Fluid Mech. **19**, 271 (1987).
[2] C. T. Tan and G. M. Homsy, "Stability of miscible displacements in porous media: Rectilinear flow," Phys. Fluids **29**, 3549 (1986).
[3] C. T. Tan and G. M. Homsy, "Simulation of nonlinear viscous fingering in miscible displacement," Phys. Fluids **31**, 1330 (1988).
[4] J.-C. Bacri, D. Salin, and R. Wouméni, "Three dimensional miscible viscous fingering in porous media," Phys. Rev. Lett. **67**, 2005 (1991).
[5] W. B. Zimmerman and G. M. Homsy, "Nonlinear viscous fingering in miscible displacement with anisotropic dispersion," Phys. Fluids A **3**, 1859 (1991).
[6] A. Rogerson and E. Meiburg, "Numerical simulation of miscible displacement processes in porous media flows under gravity," Phys. Fluids A **5**, 2644 (1993).
[7] M. Czok, A. M. Katti, and G. Guiochon, "Effect of sample viscosity in high-performance size-exclusion chromatography and its control," J. Chromatogr. **550**, 705 (1991).
[8] D. Cherrak, E. Guernet, P. Cardot, C. Herrenknecht, and M. Czok, "Viscous fingering: a systematic study of viscosity effects in methanol-isopropanol systems," Chromatographia **46**, 647 (1997).
[9] C. B. Castells and R. C. Castells, "Peak distortion in reversed-phase liquid chromatography as a consequence of viscosity differences between sample solvent and mobile phase," J. Chromatogr. A **805**, 55 (1998).
[10] B. S. Broyles, R. A. Shalliker, D. E. Cherrak, and G. Guiochon, "Visualization of viscous fingering in chromatographic columns," J. Chromatogr. A **822**, 173 (1998).
[11] M. L. Dickson, T. T. Norton, and E. J. Fernandez, "Chemical imaging of multicomponent viscous fingering in chromatography," AIChE J. **43**, 409 (1997).
[12] E. J. Fernandez, T. T. Norton, W. C. Jung, and J. G. Tsavalas, "A column design for reducing viscous fingering in size exclusion chromatography," Biotechnol. Prog. **12**, 480 (1996).
[13] T. T. Norton and E. J. Fernandez, "Viscous fingering in size exclusion chromatography: insights from numerical simulation," Ind. Eng. Chem. Res. **35**, 2460 (1996).
[14] A. De Wit, Y. Bertho, and M. Martin, "Viscous fingering of miscible slices," Phys. Fluids **17**, 054114 (2005).
[15] C.-Y. Chen and S.-W. Wang, "Miscible displacement of a layer with finite width in porous media," Int. J. Numer. Methods Heat Fluid Flow **11**, 761 (2001).
[16] S. R. D. Lunn, and B. H. Kueper, "Manipulation of density and viscosity for the optimization of DNAPL recovery by alcohol flooding," J. Contam. Hydrol. **38**, 427 (1999).
[17] V. Kretz, P. Berest, J. P. Hulin, and D. Salin, "An experimental study of the effects of density and viscosity contrasts on macrodispersion in porous media," Water Resour. Res. **39**, 1032 (2003).
[18] C. Y. Jiao and H. Hötzl, "An experimental study of miscible displacements in porous media with variation of fluid density and viscosity," Transp. Porous Media **54**, 125 (2004).
[19] T. C. Flowers and J. R. Hunt, "Viscous and gravitational contributions to mixing during vertical brine transport in water-saturated porous media," Water Resour. Res. **43**, W01407 (2007).
[20] A. H. Nayfeh, "Stability of liquid interfaces in porous media," Phys. Fluids **15**, 1751 (1972).
[21] W. B. J. Zimmerman, *Process Modelling and Simulation with Finite Element Methods* (World Scientific, Singapore, 2004).
[22] G. Guiochon, A. Felinger, D. G. Shirazi, and A. M. Katti, *Fundamentals of Preparative and Nonlinear Chromatography* (Elsevier-Academic, San Diego, 2006).
[23] Y. C. Yortsos, "The relationship between immiscible and miscible displacement in porous media," AIChE J. **33**, 1912 (1987).